

Chelating Resins VI: Chelating Resins of Formaldehyde Condensed Phenolic Schiff Bases Derived from 4,4'-Diaminodiphenyl Ether with Hydroxybenzaldehydes—Synthesis, Characterization, and Metal Ion Adsorption Studies

S. SAMAL, R. R. DAS, R. K. DEY, S. ACHARYA

Department of Chemistry, Ravenshaw College, Cuttack 753 003, India

Received 1 January 1999; accepted 14 October 1999

ABSTRACT: Phenolic Schiff bases derived from *o*-, *m*-, and *p*-hydroxybenzaldehydes and 4, 4'-diaminodiphenyl ether were subjected to polycondensation reaction with formaldehyde. The resins were found to form polychelates readily with several metal ions. The materials were characterized by elemental analysis, GPC, IR, UV-Vis, ¹H-NMR, XRD, and thermal analyses like TG, DTG, and DSC studies. The ¹H-NMR spectra of the resins provided evidence of polycondensation with well-defined peaks for bridging methylene and terminal methylol functions. The metal-ligand bonds were registered in the IR spectra of the polychelates. The thermal analysis data provided the kinetic parameters like activation energy, frequency factor, and entropy changes associated with the thermal decomposition. These data indicated the resins to be more stable than the polychelates. The DSC and XRD data indicated that the incorporation of metal ions significantly enhanced the crystallinity of the polymers. The resins could adsorb several metal ions from dilute aqueous solutions. Adsorption characteristics of the resins towards Cu(II) and Ni(II) were studied spectrophotometrically both in competitive and noncompetitive conditions. The effects of pH, contact time, quantity of the sorbent, concentration of the metal ions in a suitable buffer medium were studied. The resins were found to be selective for Cu(II) leading to its separation from a mixture of Cu(II) and Ni(II). © 2000 John Wiley & Sons, Inc. *J Appl Polym Sci* 77: 967–981, 2000

Key words: chelating resins; polychelates; characterization; metal ion uptake

INTRODUCTION

The chelate forming polymeric ligands characterized by reactive functional groups containing O, N, S, and P donor atoms and capable of coordinating to different metal ions have been exten-

sively studied.¹ The materials most often show preferential selectivity towards certain metal ions facilitating their use for preconcentration and separation of trace metal ions from saline and nonsaline water.²

Several phenol–formaldehyde condensation polymers have been synthesized and used in metal ion adsorption studies. Zigon et al.^{3,4} synthesized resorcinol–formaldehyde–crotonaldehyde resin in different media, and characterized the polymers. Parmer and coworkers⁵ synthesized resacetophenone–formaldehyde resin in acidic

Correspondence to: S. Samal, Applied Macromolecular Chemistry Laboratory, Department of Material Sciences and Engineering, Kwangju Institute of Science & Technology, 1 Oriyong-dong, Puk-gu, Kwangju 500-712, South Korea.

Journal of Applied Polymer Science, Vol. 77, 967–981 (2000)
© 2000 John Wiley & Sons, Inc.

medium and studied its chelation ion-exchange properties. Moyers and Fritz⁶ condensed *m*-phenylenediamine tetraacetic acid with resorcinol and formaldehyde to get a resin containing two iminodiacetic acid functional groups anchored to a benzene ring, and used the resin to separate Co(II) and Ni(II) in a gravity flow column. Several authors^{7,8} studied resorcinol–formaldehyde oxime polymers and found the resins to be very selective for heavy metal ions. Condensation polymerization of phenol–formaldehyde–piperazine resulted in a resin selective for Cu(II).^{9,10}

Schiff bases having multidentate coordination sites are known to form complexes with transition metal ions readily.¹¹ When present in a polymeric matrix, they are expected to show affinity and selectivity towards these metal ions at an appropriate pH. This led us to synthesize phenolic Schiff bases by condensing several aliphatic and aromatic diamines with phenolic carbonyls, or conversely, dicarbonyls with aminophenols. We have reported that a number of these Schiff bases could be condensed readily with formaldehyde and furfuraldehyde.¹² In the reaction conditions set for polycondensation the azomethine bonds (C=N) of the Schiff bases did not undergo hydrolytic cleavage. As a part of our on going research, the present communication deals with the synthesis of formaldehyde-condensed phenolic Schiff bases of 4,4'-diaminodiphenyl ether (DDE) and *o*-, *m*-, *p*-hydroxy benzaldehydes (*o*-, *m*-, *p*-HB), their characterization, and metal ion uptake behavior towards Cu(II) and Ni(II).

EXPERIMENTAL

Reagents

All the starting materials such as *o*-, *m*-, *p*-hydroxybenzaldehydes, 4,4'-diaminodiphenyl ether (Merck, Germany), were recrystallized from ethanol before use. The sulphate and nitrate salts of Cu(II) and Ni(II), paraformaldehyde and all other chemicals and solvents were of AnalaR/GR grade (Merck/BDH, India), and were used as received. The buffers used to control the pH of the solution were acetic acid–sodium acetate (pH 3.42–5.89), disodium hydrogen phosphate–potassium dihydrogen phosphate (pH 5–8), and ammonium hydroxide–ammonium chloride (pH 8–10).

Preparation of Schiff Base Monomers

The Schiff base monomers *o*-, *m*-, *p*-hydroxybenzaldehyde–4,4'-diaminodiphenyl ether (*o*-, *m*-, *p*-

HB-DDE) were synthesized by reacting 2 g (0.01 mol) of 4,4'-diaminodiphenyl ether dissolved in 10 mL of methanol with 2.24 g (0.02 mol) of hydroxy benzaldehyde in the presence of 0.5 g of anhydrous sodium acetate. The mixture was refluxed for 1 h at 60°C, poured into ice-cold water, and allowed to stand for 30 min. The precipitated solids were filtered, washed repeatedly in demineralized water, and recrystallized from methanol. The *o*- and *p*-HB-DDE were isolated as yellow crystalline solids, and the *m*-HB-DDE was isolated as a brown glassy material. *o*-HB-DDE: ¹H-NMR (300 MHz, DMSO *d*₆) δ 6.48–6.51 (d), 6.58–6.26(d), 7.4–7.76(m), 8.9(s); IR (KBr pellet) ν 3400, 1610, 1570, 1480, 1455, 1405, 1275, 740 cm⁻¹; Anal. % Calcd.: C 76.38, H 4.93, N 6.85; Found C 76.36, H 4.92, N 6.84; *p*-HB-DDE: ¹H-NMR (300 MHz, DMSO *d*₆) δ 6.74–6.77 (dd), 6.83–6.86(d), 7.23–7.26(dd), 7.71–7.74(d), 8.47(s); IR (KBr pellet) ν 3300, 1600, 1510, 1490, 1250, 835, 715 cm⁻¹; Anal. % Calcd.: C 76.38, H 4.93, N 6.85; Found C 76.25, H 4.92, N 6.78.

Preparation of the Resins

The Schiff base monomer (1 g, 0.0024 mol) suspended in 20 mL water at 40°C was dissolved in minimum volume of 1 *M* NaOH. Paraformaldehyde in 1 : 2 molar ratio was added, and the mixture was refluxed in an oil bath at 120–130°C for 2 h. The insoluble resin was filtered, washed repeatedly with distilled water, and dried at 70°C. The yield of all the three resins *o*-, *m*-, and *p*-HB-DDE-HCHO (Fig. 1) was found to exceed 70%. The dry resin was powdered and suspended over water at pH 4 overnight. It was filtered, washed in large excess of water, followed by methanol, and dried in a vacuum at 70°C. Hydroxybenzaldehydes were also condensed with HCHO yielding *o*-, *m*-, *p*-HB-HCHO resins. The IR and ¹H-NMR of these resins were compared with those of the Schiff base resins to find out if the Schiff base monomers suffered hydrolysis under the reaction conditions set for polymerization. *o*-HB-DDE-HCHO: ¹H-NMR (300 MHz, DMSO *d*₆) δ 3.1–3.9 (m), 4.2–5.1(m), 6.5–8(m), 8.9(s); IR (KBr pellet) ν 3350, 1610, 1490, 1400, 1275, 740 cm⁻¹; UV-Vis (CHCl₃) λ_{max}/nm 239.2, 268, 349.6; Anal. % Found C 64.1, H 4.56, N 4.3; [η]_{int} dL/g 0.133; *m*-HB-DDE-HCHO: ¹H-NMR (300 MHz, DMSO *d*₆) δ 3.2–3.7 (m), 4.4–5.3(m), 6.1–7.5(m), 8.5(s); IR (KBr pellet) ν 3350, 1600, 1480, 1215, 810 cm⁻¹; UV-Vis (CHCl₃) λ_{max}/nm 380.8, 480.8, 551.2; Anal. % Found C 62.9, H 4.56, N 4.56; [η]_{int}

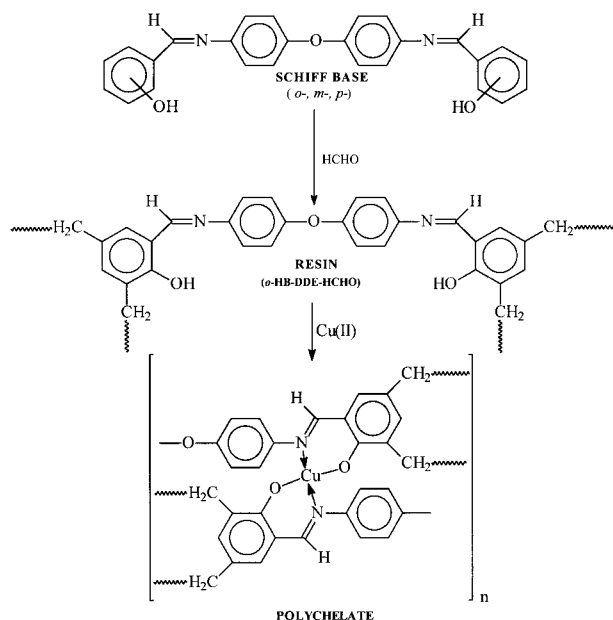


Figure 1 Reaction scheme showing coordination sites of the resin for metal binding.

dL/g 0.145; \bar{M}_n 1058, \bar{M}_w 1544, \bar{M}_z 2586, \bar{M}_{z+1} 4559, Polydispersity 1.459; *p*-HB-DDE-HCHO: $^1\text{H-NMR}$ (300 MHz, DMSO d_6) δ 3.8–5.3(m), 5.5(s), 6.47.9(m), 8.5(s); IR (KBr pellet) ν 3385, 1660, 1470, 1230, 820 cm^{-1} ; UV-Vis (CHCl_3) $\lambda_{\text{max}}/\text{nm}$ 257.6, 271.2, 386.4; Anal. % Found C 66.8, H 4.8, N 4.3; $[\eta]_{\text{int}}$ dL/g 0.136; \bar{M}_n 1127, \bar{M}_w 1834, \bar{M}_z 3119, \bar{M}_{z+1} 5035, Polydispersity 1.626.

Preparation of the Polychelates

To 100 mg of the dry resin (100 mesh, ASTM) suspended over methanol, 10 mL of metal salt (0.15 M) in water was added. The mixture was stirred for 2 h at 40°C. It was filtered, washed in distilled water, followed by petroleum ether, and dried in a vacuum at 70°C. *o*-HB-DDE-HCHO-Cu(II): IR (KBr pellet) ν 3300, 1605, 1040, 980, 730, 645, 560 cm^{-1} ; UV-Vis $\lambda_{\text{max}}/\text{nm}$ 240, 348.8; Anal. Found C 55.3, H 3.98, N 3.9; *m*-HB-DDE-HCHO-Cu(II): IR (KBr pellet) ν 3200, 1030, 970, 635, 560 cm^{-1} ; UV-Vis $\lambda_{\text{max}}/\text{nm}$ 348, 550.4, 636; Anal. Found C 58.4, H 3.4, N 3.45; *m*-HB-DDE-HCHO-Ni(II): IR (KBr pellet) ν 3200, 1590, 1400, 1215 cm^{-1} ; Anal. Found C 56.3, H 2.9, N 2.98; *p*-HB-DDE-HCHO-Cu(II): IR (KBr pellet) ν 3300, 1600, 1200, 1140, 1040, 980, 810, 640, 560 cm^{-1} ; UV-Vis $\lambda_{\text{max}}/\text{nm}$ 332.8; Anal. % Found C 58.5, H 4.2, N 4.05; *p*-HB-DDE-HCHO-Ni(II): IR (KBr pellet) ν 3300, 1600, 1400, 1200, 810, 640, 560

cm^{-1} ; UV-Vis $\lambda_{\text{max}}/\text{nm}$ 332.8; Anal. % Found C 56.7, H 4.15, N 3.45.

Measurements

The intrinsic viscosity of the resins dissolved in dimethyl sulphoxide (DMSO) was determined by viscometry using an Ubbelohde suspended level viscometer. A Waters Gel Permeation Chromatography equipment employing polystyrene as the reference standard was used to determine the molecular weight of the resins. The elemental analysis was carried out in a Carlo Erba 1108 elemental analyzer. The IR spectra were recorded on a Perkin-Elmer spectrometer model 577 in the range of 4000–200 cm^{-1} in the KBr phase. The $^1\text{H-NMR}$ spectra were recorded in DMSO d_6 solvent in 400/300 MHz FT NMR (Bruker WM 400/DRX 300) instruments. The electronic spectra of the resins dissolved in CHCl_3 were recorded on a Perkin-Elmer Lambda 15 spectrophotometer. The TG (Du Pont 951) and DSC (Du Pont 9900) of the materials were recorded up to 700°C at a heating rate of 10°C/min in a nitrogen atmosphere. The wide-angle X-ray diffractograms (2θ range of 4–35°, scanning rate of 0.05/1.25 min) of the resins and polychelates were obtained from a PW 1820 diffractometer operating at 40 kV and 30 mA and using Cu- K_α radiation. The estimation of the metal ion concentration in the dilute aqueous solutions and the pH measurements were made using a Systronics Digital UV-Vis Spectrophotometer model 116 and Systronics Digital pH Meter model 335, respectively.

RESULTS AND DISCUSSION

Solubility

The freshly prepared resin (100 mesh, 10 mg) was suspended over 5 mL of the chosen solvent at room temperature, and the solubility was checked after 24 h (Table I). All the three resins *o*-, *m*-, and *p*-HB-DDE-HCHO were found to be completely insoluble in water; they were partially soluble in CHCl_3 and CCl_4 but completely soluble in DMSO. The resins *m*-, and *p*-HB-DDE-HCHO were soluble in THF, but *o*-HB-DDE-HCHO was only partially soluble. All the polychelates were found to be partially soluble in DMSO, THF, CHCl_3 and insoluble in most other solvents. The poor solubility of the polychelates was ascribed to alter-

ation in polymer polarity and intrapolymer cross-linking¹⁰ as well as increase in crystallinity.¹³

Intrinsic Viscosity and Molecular Weight

The specific viscosity, η_{sp} , of the resins dissolved in DMSO was determined using an Ubbelohde viscometer. From the Huggins plot of η_{sp}/C vs. C , where C is the concentration of the resin solution in g/dL; the intrinsic viscosity, $[\eta]_{int}$, for the resins, found by extrapolation of the plot to zero concentration as well as by regression analysis of the data. It was found to vary between 0.132 to 0.145 dL/g. Chen et al.¹⁴ have synthesized Schiff base coordination polymers and observed the intrinsic viscosity of the polymers to lie nearly in this range.

The molecular weight of the resins was determined by GPC from THF solutions using narrow standard polystyrene as a reference. It was seen that condensation of HCHO with *p*-HB-DDE resulted in a slightly higher molecular weight polymer than with *m*-HB-DDE. The GPC of *o*-HB-DDE-HCHO could not be run, as the resin was not completely soluble in THF. Apparently, polycondensation of HCHO with *o*-HB-DDE is relatively more effective leading to a highly crosslinked polymer than with the other two Schiff bases.

Spectral Studies

Infrared Spectra

The IR spectra of the *o*, *m*- and *p*-hydroxybenzaldehydes–formaldehyde resins (*o*-, *m*-, and *p*-HB-HCHO) showed strong C=O absorption, which was absent in the resins *o*-, *m*-, and *p*-HB-DDE-HCHO, indicating that the Schiff bases did not undergo hydrolysis under the reaction conditions set for condensation polymerization.

The C=C, C=N stretches, and other characteristic absorptions including those in the finger print region for the Schiff bases were sharp. The spectra of the corresponding resins showed broad absorptions and a number of vibrations in the finger print region of the Schiff base vanished or diminished in intensity. In *o*-HB-DDE-HCHO-Cu(II) polychelate, the C=N stretch shifted by 5 cm^{-1} towards lower frequency region and Ph—O absorption was registered at lower frequency, but merged with SO_4^{2-} group vibrations. In the case of *m*- and *p*-HB-DDE-HCHO-Cu(II), there was a shift of the phenolic C—O from its position in the resin, but the C=N shift was not significant. Several authors have made similar observations.^{14–16}

In addition, in the IR spectra of all the three polychelates, prominent absorption at 640–580 and 560–550 cm^{-1} were observed, which were assigned to the M—O and M—N bonds, respectively. Ueno and Martell^{11a} have made extensive band assignments for the metal chelate compounds of *bis*-acetylacetonate–ethylenediimine and *bis*-salicylaldehyde–ethylenediimine and have suggested that the metal–ligand stretching vibrations in these Schiff base complexes appear in the range 640–500 cm^{-1} for the M—O and 580–430 cm^{-1} for the M—N bonds.

In addition to phenolic oxygen and aldimine nitrogen binding the metal ion, there is evidence that the counteranion SO_4^{2-} from CuSO_4 used to synthesize *o*-, *m*-, and *p*-HB-DDE-HCHO-Cu(II) is acting as a bridging group between metal ions ($\text{Cu}^{2+}\text{—O—SO}_2\text{—O—Cu}^{2+}$). This conclusion is based on the characteristic modes of sulphate group vibrations at 1140–1080 (broad), 1030, and 980 cm^{-1} . Nakamoto et al.¹⁷ studied bridged sulphato-complexes of Co(II) and reported similar observations.

In case of Ni(II) polychelates the M—O and M—N bands were not sharp and no shift was noticed in the phenolic C—O and C=N absorptions. This observation is demonstrative of lowered preference of the resin for Ni^{2+} than for Cu^{2+} . The Ni(II) polychelates also showed a strong absorption band at 1400 cm^{-1} , which is characteristic of a free NO_3^- from $\text{Ni}(\text{NO}_3)_2$ used for polychelate synthesis.¹⁸ Both Cu(II) and Ni(II) polychelates also showed absorptions at ~3400, 900, and 400 cm^{-1} indicating the presence of coordinating as well as lattice water.¹⁹

UV-Visible Spectra

The UV-Vis spectrum of the resin *o*-HB-DDE-HCHO showed multiple peaks at 239.2, 268, and 349.6 nm. No absorption could be seen in the d–d transition region of the Cu(II)-polychelate. In case of the resin *p*-HB-DDE-HCHO, absorptions were seen at 257.6, 271.2, and 386.4 nm. The polychelate *p*-HB-DDE-HCHO-Cu(II) had a single absorption at 332.8 nm. The resin, *m*-HB-DDE-HCHO had a better solubility in different solvents compared to the other two resins. Its Cu(II) polychelate was fairly soluble in CHCl_3 and the UV-Vis spectrum showed absorptions at 348, 550.4, and 636 nm. The absorption at 636 nm ($\bar{\nu} = 15,720 \text{ cm}^{-1}$) was ascribed to ${}^2E_g \rightarrow T_{2g}$ transition for Cu(II) present in a distorted octahedral ligand environment.²⁰

¹H-NMR Spectra

The characteristic aldehyde proton peaks are absent in the ¹H-NMR spectra of the Schiff base monomers and their resins indicating that the C=N bonds of Schiff bases remained intact in the conditions set for polycondensation. For the Schiff base *o*-HB-DDE, the aldimine proton was recorded at 8.9 ppm. A set of multiplets in the range 6.4 to 7.4 ppm was due to aromatic protons. The *p*-HB-DDE Schiff base registered aromatic protons in the range 6.5 to 7.7 ppm, and the aldimine proton at 8.4 ppm. The sharp well-resolved peaks of the Schiff bases turned to broad overlapping multiplets in the resins. The resin *o*-HB-DDE-HCHO registered two broad absorptions in the range 3.1–3.9 ppm and 4.2–5.1 ppm ascribed to bridging methylene groups and hydrogen bonded terminal methylol functions, respectively. The spectral features of *m*-HB-DDE-HCHO and *p*-HB-DDE-HCHO exhibited near identical trends as those of *o*-HB-DDE-HCHO.

A comparison of the aromatic proton peak area of the resin and that of the DMSO *d*₆ solvent impurity peak was made, leading to the determination of the average molecular mass of the resins. The peak area ratio of aromatic protons of resins to the DMSO CH₃ protons (solvent impurity) was observed to be ~4.5 : 1, 4 : 1, and 5 : 1 for the *o*-, *m*-, and *p*-HB-DDE-HCHO resins, which by empirical calculation provided the average molecular mass of 1035, 920, and 1150, respectively. These results closely agreed with the \bar{M}_n data obtained from GPC studies.

Thermal Analyses Studies

Thermogravimetric Analysis

The TG traces showed the decomposition pattern for resin *o*-HB-DDE-HCHO and its Cu(II) complex (Fig. 2). It was observed that up to 200°C the resin lost only 2.78% of its original weight, which could be mostly adsorbed water. The weight loss in the range of 200–400°C was 30%. The temperature of maximum rate of decomposition for the resin was 285.68°C, rate of weight loss being 0.3589%/°C at this temperature. Between 400–700°C the weight loss was 60.71%, and the rate of weight loss at the peak decomposition temperature of 598.29°C was 0.4436 %/°C. The char yield at 700°C was 6.37%.

The Cu(II) polychelate *o*-HB-DDE-HCHO-Cu(II) lost 9.7% of its original weight within 90°C, with peak decomposition at 67.31°C at a rapid

rate of 0.4481%/°C. This is ascribed to desorption of methanol, the solvent used for the synthesis of the polychelate. Between 90 to 140°C, a second decomposition stage followed with the peak rate of decomposition of 0.3943%/C at 107.69°C, indicating the loss of water molecule present in the lattice either in the free form, or as coordinated to the metal ion. In this range, the weight loss was 9.48%. Thus, within 200°C, the polychelate lost almost 20% of its weight. Between 200–400°C, the weight loss was 12.22% at a rate of 0.1945%/°C, with a peak decomposition temperature of 254.27°C. Beyond 400°C, the weight loss was slower than the resin. While the resin lost 60% between 400–700°C, the polychelate lost only 14.37%. The char yield at 700°C for the polychelate was 53.76%, due mostly to the nonvolatile metal oxide.

The polychelates suffered rapid decomposition at lower temperature. After desorption of the solvents, the first peak decomposition temperatures for the resin was higher than that of the polychelate. This led to the conclusion that the polychelates are less stable than the corresponding resins. We have studied the thermal decomposition of a number of resins derived from phenolic Schiff bases¹² and observed a similar decrease in thermal stability of the polychelates over that of the corresponding resins. The metal ions in the polychelates were stated to be responsible in catalyzing the thermal decomposition resulting in the molecular framework to undergo fragmentation.

Evaluation of Kinetic Parameters

To compare the relative thermal stability of the resins and the polychelates and draw conclusions unambiguously, the kinetic parameters for the thermal decomposition of the materials were evaluated using several integral methods such as:

COATS – REDFERN²¹

$$\ln[g(\alpha)/T^2] = \ln[AR/\beta E(1 - 2RT/E)] - E/RT \quad (1)$$

VAN KREVELEN²²

$$\ln[g(\alpha)] = \ln[A/\beta(0.368/T_m)^{E/RT_m}(E/RT_m + 1)^{-1}] + (E/RT_m + 1)\ln T \quad (2)$$

BROIDO²³

$$\ln[g(\alpha)] = \ln[A/\beta \times (R/E)T_m^2] - (E/R) \times 1/T \quad (3)$$

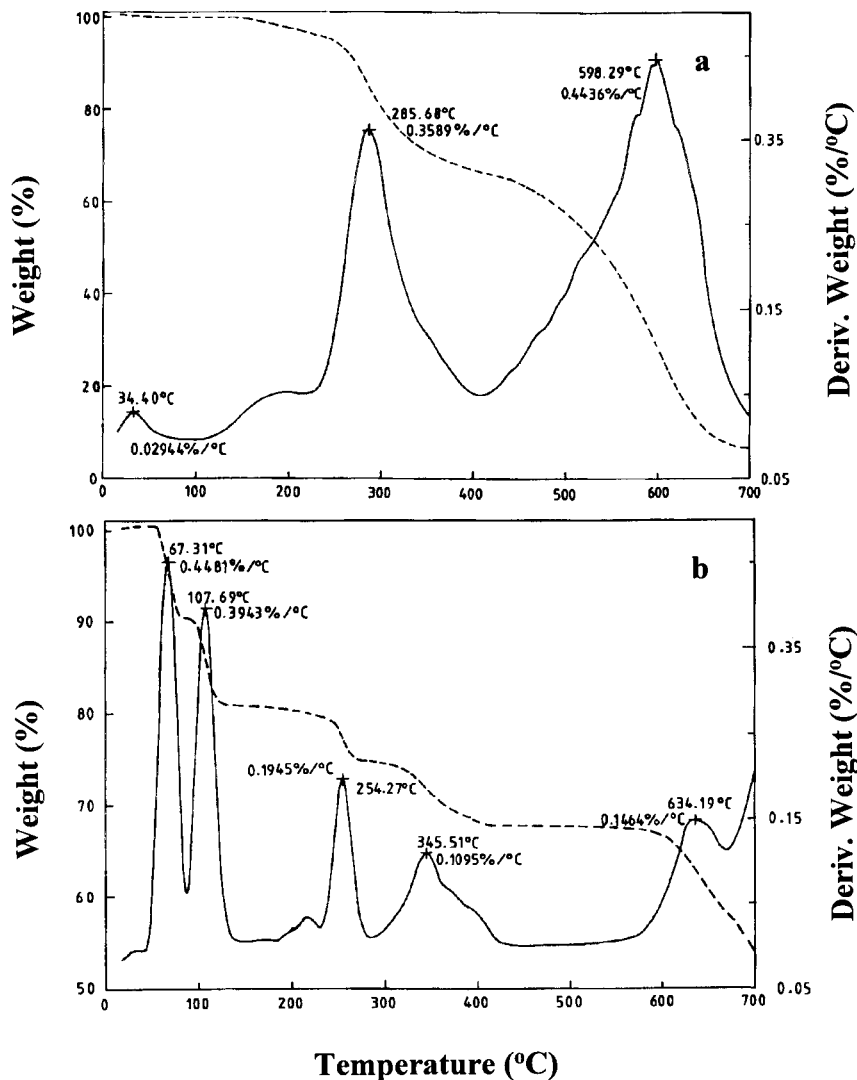


Figure 2 TG-DTG traces of (a) *o*-HB-DDE-HCHO and (b) *o*-HB-DDE-HCHO-Cu(II).

where $\alpha = [W_o - W]/[W_o - W_f]$, W_o = initial weight, W = weight at temperature T , W_f = final weight, β = heating rate ($\text{deg} \cdot \text{min}^{-1}$), T_m = temperature of maximum rate of weight loss ($^{\circ}\text{K}$), E = activation energy (kcal), A = frequency factor (s^{-1}), and $g(\alpha)$ = a function of α .

The activation energy E and the frequency factor A were computed for the different models from the slope and the intercept of the plot of $\ln[g(\alpha)/T^2]$ vs. $1/T$ for the Coats and Redfern, $\ln[g(\alpha)]$ vs. $\ln T$ for the Van Krevelen, and $\ln[g(\alpha)]$ vs. $1/T$ for the Broido models after linear regression analysis of the data (Fig. 3). The entropy of activation ΔS ($\text{cal} \cdot \text{K}^{-1} \cdot \text{mol}^{-1}$) was calculated using the relation $A = (kT_m/h)(e^{\Delta S/R})$ where k is the Boltzmann constant ($0.32944 \times 10^{-23} \text{ cal} \cdot \text{K}^{-1}$), h , the Planck's

constant ($1.5836 \times 10^{-34} \text{ cal} \cdot \text{s}$), and R , the gas constant ($1.9872 \text{ cal} \cdot \text{mol}^{-1} \cdot \text{K}^{-1}$). The data are furnished in Table II. For different models the activation energy of the resins were found to be more than that of the polychelates, indicating the resins to be more stable than the polychelates.

The three different models were consistently valid in different temperature ranges, as seen from the linear regression plots (Fig. 3), R^2 values, and the kinetic energy data (Table II). For example, for *o*-HB-DDE-HCHO, the Coats-Redfern model fits in nicely for the temperature ranges 130–610, as well as 210–400 and 420–660°C. Further, it is seen that when applied to different temperature ranges, the models still furnished kinetic parameters, which indicated

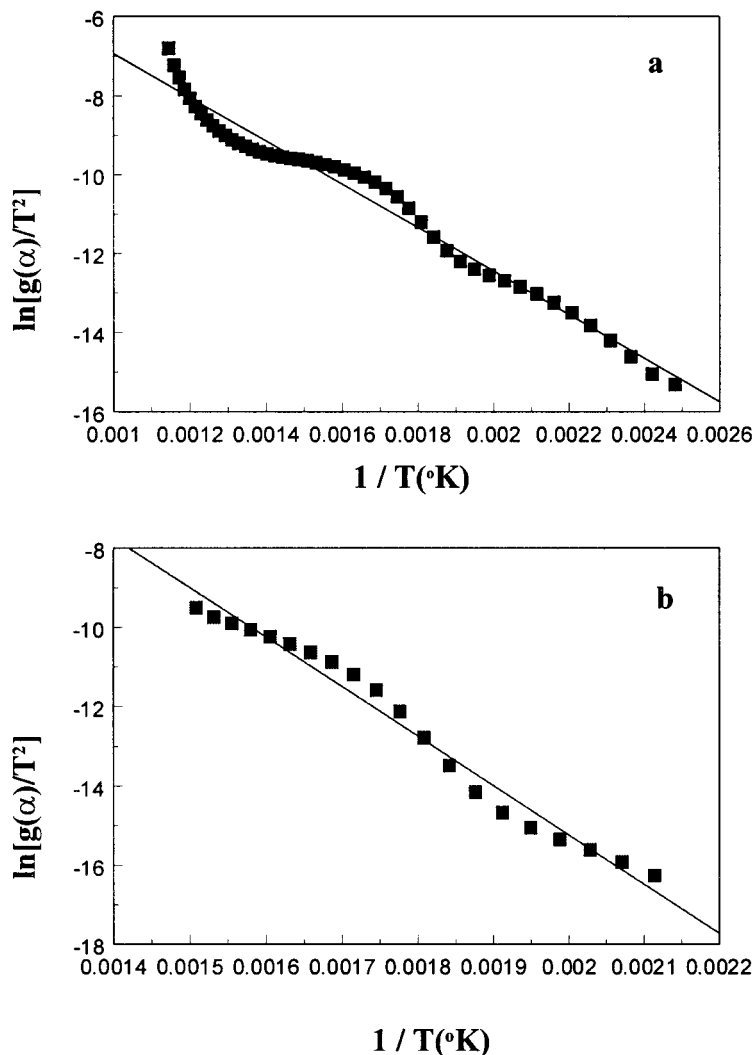


Figure 3 Coates and Redfern plot of $\ln [g(\alpha)/T^2]$ vs. $1/T$ for *o*-HB-DDE-HCHO for the range (a) 130–610 and (b) 210–400°C, demonstrating validity of the model in different temperature ranges.

that the resins are more stable than the polychelates.

DSC Study

The DSC pattern of the resin *o*-HB-DDE-HCHO and its Cu(II) polychelate showed in Figure 4 exhibit significant differences. The glass transition temperature of the resin was noticed at 85°C followed by a very weak crystallization peak, beyond which the resin melts at 197.62°C followed by exothermic decomposition reactions at a peak maximum of 230.95°C. On the other hand, the Cu(II)-polychelate showed three endothermic transitions closely placed with minima at 102.38, 114.29, and 133.33°C.

Methanol and water molecules either hydrogen bonded to the phenolic oxygen and azomethine nitrogen and/or coordinated to the metal ions are present in the complex molecular matrix. The three endotherms in the polychelate could be related to structural changes consequent upon the loss of these lattice or coordinated solvent molecules. The glass transition was not noticed for the polychelate, indicating it to be appreciably crystalline, indicated further by the sharp melting temperature at 271.43°C.

XRD Study

The XRD pattern of the resin *o*-HB-DDE-HCHO and the Cu(II)-polychelate is presented in Figure

Table I Color and Solubility

Compound	Color	Solubility in Different Solvents ^a						
		H ₂ O	CH ₃ OH	CCl ₄	CHCl ₃	DMF	DMSO	THF
<i>o</i> -HB-DDE	Yellowish white	–	±	+	+	+	+	+
<i>o</i> -HB-DDE-HCHO	Yellow	–	±	±	±	+	+	–
<i>o</i> -HB-DDE-HCHO-Cu(II)	Light blue	–	–	–	–	±	±	±
<i>o</i> -HB-DDE-HCHO-Ni(II)	Black	–	–	–	–	±	±	±
<i>m</i> -HB-DDE	Yellowish white	–	±	+	+	+	+	+
<i>m</i> -HB-DDE-HCHO	Brown	–	±	±	±	+	+	+
<i>m</i> -HB-DDE-HCHO-Cu(II)	Chocolate	–	–	–	–	±	±	±
<i>m</i> -HB-DDE-HCHO-Ni(II)	Dark brown	–	–	–	–	±	±	±
<i>p</i> -HB-DDE	Yellowish white	–	±	+	+	+	+	+
<i>p</i> -HB-DDE-HCHO	Yellow	–	±	±	±	+	+	+
<i>p</i> -HB-DDE-HCHO-Cu(II)	Light green	–	–	–	–	±	±	±
<i>p</i> -HB-DDE-HCHO-Ni(II)	Reddish brown	–	–	–	–	±	±	±

^a (+) Soluble, (±) Partially soluble, (–) Insoluble.

5. The resin exhibited one strong reflection at (2θ) 19.2° and a weaker reflection at 24.5°. Yang and Chen¹³ reported that polymers having *p*-phenylene units containing *bis*(phenoxy)benzene group exhibited one strong peak reflection at around 20°, and weaker reflection at around 27°, and assigned these reflections to the crystalline nature of the polymers.

The polychelate exhibited a number of additional reflection planes, the most intense reflec-

tion appearing at 18.9. This is assignable to a significant increase in crystallinity of the polymer consequent upon coordination to the metal ion. From a comparison of the peak area it was observed that the polychelate could be nearly 6.667 times more crystalline than the resin. The observed increase in the number of reflections and intensities could also be the result of an increase in electron density due to metal ion uptake.

Table II Kinetic Parameters

Compounds	Temp. Range (°C)	T_{\max} (K)	Methods ^a	R^2	E (kcal)	A (s ⁻¹)	ΔS (CalK ⁻¹ mol ⁻¹)
<i>o</i> -HB-DDE-HCHO	130–610	558.68	CR	0.975444	10.905	1.32E+04	–40.939
		558.68	VK	0.945754	8.11	3.24E+01	–52.88
		558.68	BR	0.963348	9.843	2.02E+02	–49.24
<i>o</i> -HB-DDE-HCHO	210–400	558.68	CR	0.978186	25.93	7.13E+09	–14.701
		558.68	VK	0.984053	13.04	7.57E+03	–42.042
		558.68	BR	0.980368	12.407	7.73E+03	–41.999
<i>o</i> -HB-DDE-HCHO	420–660	871.29	CR	0.865774	27.648	1.49E+08	–23.277
		871.29	VK	0.966771	4.298	3.65E–01	–62.679
		871.29	BR	0.952906	5.425	6.28E–01	–61.601
<i>o</i> -HB-DDE-HCHO-Cu(II)	130–610	527.27	CR	0.938785	3.914	1.28E+01	–54.607
		527.27	VK	0.943499	1.375	8.79E–02	–64.51
		527.27	BR	0.939998	1.702	1.46E–01	–63.509
<i>o</i> -HB-DDE-HCHO-Cu(II)	180–420	527.27	CR	0.955957	2.462	1.59E+01	–54.179
		527.27	VK	0.967646	0.4	2.71E–02	–66.848
		527.27	BR	0.96065	1.493	8.06E–02	–64.684

^a CR: Coats-Redfern, VK: Van Krevelen, BR: Broido.

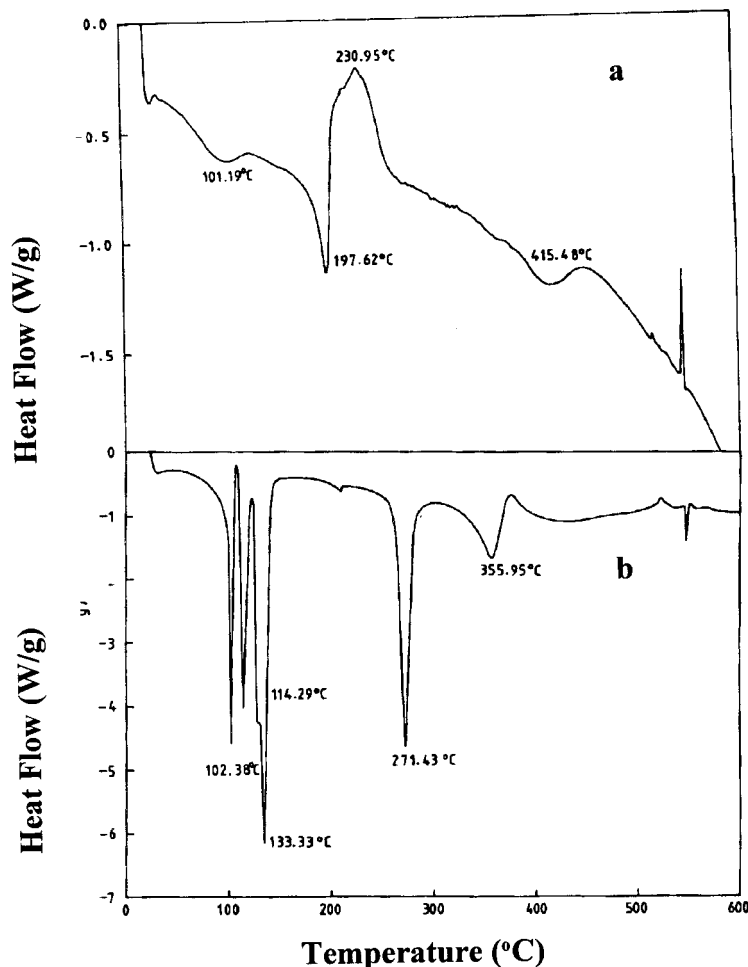


Figure 4 DSC traces of (a) *o*-HB-DDE-HCHO and (b) *o*-HB-DDE-HCHO-Cu(II).

Metal Ion Uptake

The metal ion uptake of the resins was determined by batch method at two different metal ion concentrations (20 and 200 $\mu\text{g mL}^{-1}$). Metal salt solutions were prepared in a buffer solution of desired pH range. To 10 mL of the metal salt solution, 100 mg of the resin of 100 mesh was added and shaken for a fixed time period in stoppered conical flasks at 30°C. The contents of the flask were filtered off, and the resin was thoroughly washed in demineralized water. The metal ion concentration in the filtrate and the washings was determined spectrophotometrically following neocuproin method for Cu(II) and dimethyl glyoxime method for Ni(II).²⁴ The experiments were carried out in duplicate each time. The percentage of metal ion adsorbed by the resin and the distribution coefficient, K_d , were calculated using the following relations:

$$\text{Metal Ion Uptake(\%)} = \frac{W_i - W_f}{W_i} \times 100 \quad (4)$$

where W_i is the μg of metal ion in solution initially present, and W_f is the μg of metal ion present in the filtrate and the washings.

Distribution Coeff., $K_d(\text{mL/g})$

$$= \frac{\text{mmol of metal on the sorbent} \times \text{mL of solution}}{\text{mmol of metal in solution} \times \text{g of resin}} \quad (5)$$

Equilibrium Time

The equilibrium time of adsorption for respective metal ions was found out by adding 100 mg of the resin of 100 mesh to 10 mL of metal ion solution prepared in acetate buffer at pH 5.6. A number of

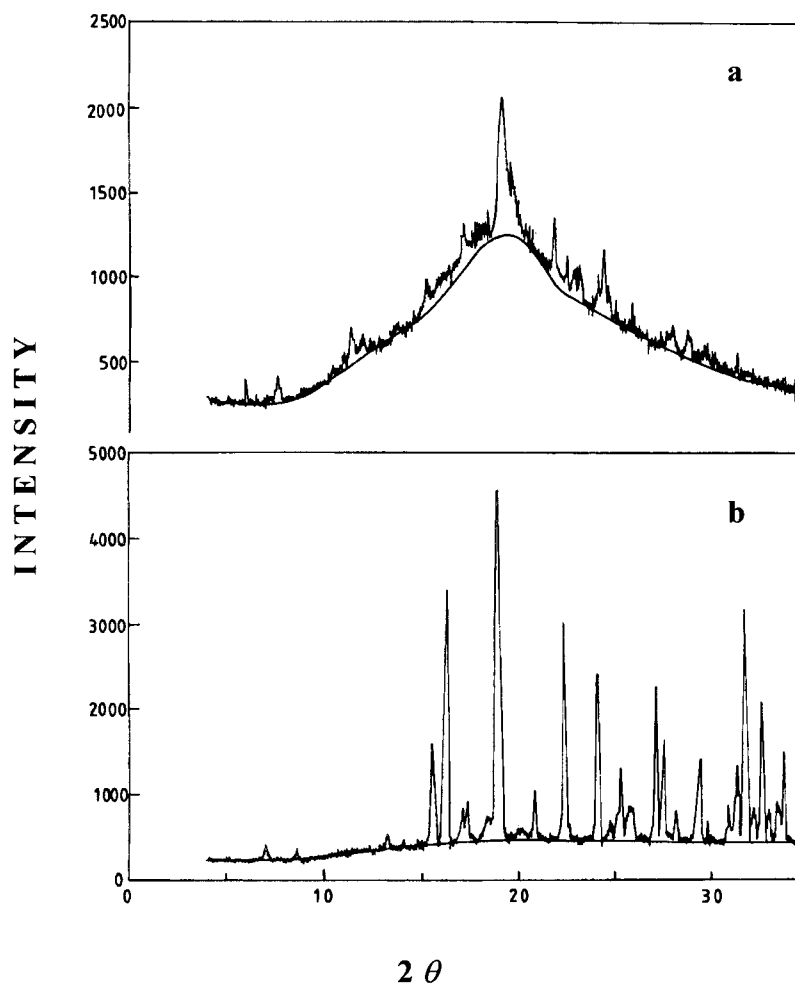


Figure 5 XRD pattern of (a) *o*-HB-DDE-HCHO and (b) *o*-HB-DDE-HCHO-Cu(II).

stoppered conical flasks containing metal ion solution and resin were stirred continuously at 30°C. The flasks were removed after regular intervals, the contents filtered off, and the amount of metal ion in the filtrate and the washings were determined.

The equilibrium time was ~ 1 h at a metal ion concentration of $200 \mu\text{g mL}^{-1}$. The resin *m*-HB-DDE-HCHO was found to be more effective than the *o*- and *p*-HB-DDE-HCHO, removing a maximum of 60% Cu(II) in 24 h [Fig. 6(a)]. When the Cu(II) concentration was decreased to $20 \mu\text{g mL}^{-1}$, the equilibrium was attained faster and within 30 min, the resin *m*-HB-DDE-HCHO absorbed nearly 99% of Cu(II) ion [Fig. 6(b)]. Thus, the rate of adsorption was relatively slow at higher metal ion concentration and fast at low metal ion concentrations. The higher adsorption efficiency of *m*-HB-DDE-HCHO is apparently due to the ease of accessibility of its coordination sites

to the metal ions, which is connected to extent of cross linking. Although the resin *o*-HB-DDE-HCHO could be easily formed with high yields, it is considerably crosslinked, rendering the coordination sites inaccessible to a great extent.

Effect of pH

The effect of variation of pH was studied at two different concentrations of the metal ions in the range of 3.42–5.89 for Cu(II) and 3.42–8.6 for Ni(II) [Fig. 7(a)–(c)]. The metal ion uptake increased significantly with increase in pH of the solution. At a concentration of $200 \mu\text{g mL}^{-1}$, the *m*-HB-DDE-HCHO resin was found to remove 66% of the metal ion at pH 5.89. At this concentration, the adsorption for Ni(II) between pH 3.42–5.89 was low, increasing steadily with a further increase in pH. At a lower concentration of $20 \mu\text{g mL}^{-1}$ [Fig. 7(c)] and at pH 5.6, nearly 100%

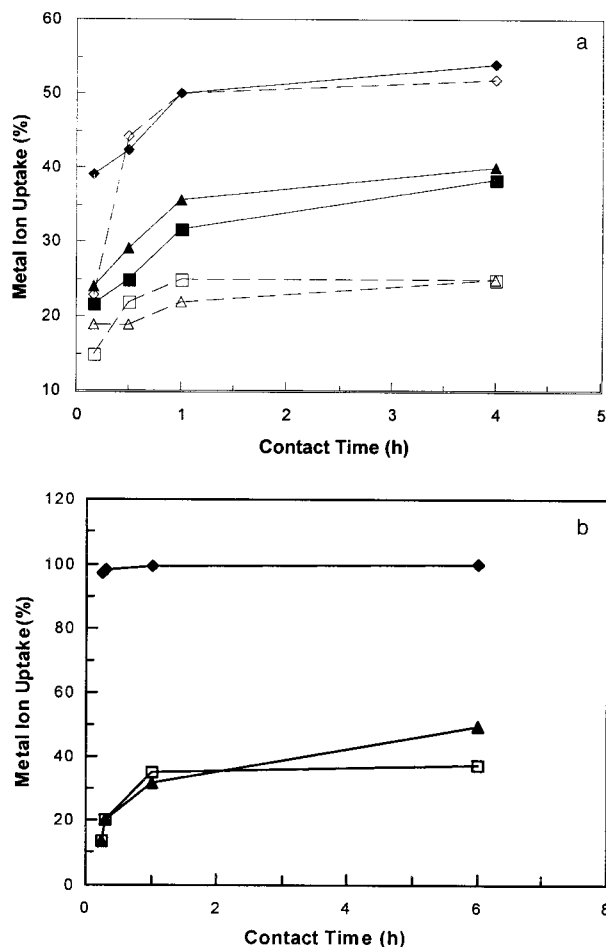


Figure 6 (a) Effect of contact time on metal ion uptakes: resin quantity—100 mg, sorbent size—100 mesh, temp. 30°C, $[M^{2+}] = 200 \mu\text{g mL}^{-1}$, uptake of Cu(II) pH 5.6: (■) *o*-, (◆) *m*-, and (▲) *p*-HB-DDE-HCHO and Ni(II) (pH 5.3): (△) *o*-, (◇) *m*-, and (□) *p*-HB-DDE-HCHO. (b) Effect of contact time on metal ion uptake: resin quantity—100 mg, sorbent size—100 mesh, temp. 30°C, $[M^{2+}] = 20 \mu\text{g mL}^{-1}$, pH 5.6, uptake of Cu(II): (□) *o*-, (◆) *m*-, and (▲), *p*-HB-DDE-HCHO.

of the Cu(II) could be removed by *m*-HB-DDE-HCHO, whereas the preference for Ni(II) at this pH was low. Adsorption studies of Cu(II) beyond pH 5.89 could not be studied due to the precipitation of Cu(II) as $\text{Cu}(\text{OH})_2$.

The preference of the resins for metal ions at a higher pH was ascribed to the ease of coordination of the phenoxide ion over that of the phenolic O—H group, and also the enhanced basicity of the C=N nitrogen, which got protonated in the acidic conditions. Lezzi and Cobianco²⁵ have reported the enhanced adsorption of Co(II) and Cu(II) at high pH values, whereas the adsorption of Hg(II) ion was not influenced.

Effect of Metal Ion Concentration

When the concentration of Cu(II) was increased in the range of 20–600 $\mu\text{g mL}^{-1}$, the extent of sorption was found to steadily decrease (Fig. 8). While nearly the entire metal ion was adsorbed by *m*-HB-DDE-HCHO resin from 10-mL solution containing 20 $\mu\text{g mL}^{-1}$, the efficiency of the resin gradually decreased with increase in metal ion concentration. Tikhomirova et al.²⁶ have observed a similar trend.

The adsorption coefficients, k_{ad} , of the resins for metal ions was computed from the Freundlich adsorption isotherm (Fig. 9):

$$\log(x/m) = \log k_{\text{ad}} + 1/n \log C \quad (6)$$

where C is the initial concentration of the metal ion in mmol, m the weight of the resin in grams, x the quantity of the metal ion adsorbed in mmol, and n a constant. For Cu(II) adsorption, the results for *o*-HB-DDE-HCHO resin are $k_{\text{ad}} = 0.332 \text{ s}^{-1}$, $n = 1.34$; for *m*-HB-DDE-HCHO, $k_{\text{ad}} = 0.356 \text{ s}^{-1}$, $n = 1.39$; and for *p*-HB-DDE-HCHO, $k_{\text{ad}} = 0.122 \text{ s}^{-1}$, $n = 1.575$. The low k_{ad} values indicate a slow adsorption rate, i.e., the equilibrium for metal ion adsorption was attained slowly. Luo and coworkers²⁷ have reported the adsorption constants for Mo(VI) and W(VI), and they associated low k_{ad} values to slow adsorption rate of metal ions.

Effect of Resin Quantity

The Cu(II) solution (10 mL, 200 $\mu\text{g mL}^{-1}$) was treated with varying amount (50–500 mg) of the resin of 100 mesh for 24 h at pH 5.89. It was observed that with increase in resin quantity, the metal ion uptake increased. Thus, 400 mg of the resin *m*-HB-DDE-HCHO could remove 100% metal ion (Table III). When the concentration of the metal ion was 20 $\mu\text{g mL}^{-1}$, 100 mg of resin was sufficient to remove almost the entire metal ion. Feng et al.²⁸ have observed that with increasing resin quantity, the percentage of metal uptake increased leading to complete removal of the metal ion.

Effect of Alkali and Alkaline Earth Metals:

To 10 mL of Cu(II) solution (200 $\mu\text{g mL}^{-1}$) containing 50 $\mu\text{g mL}^{-1}$ of Na^+ , K^+ , or Mg^{2+} (common anion: SO_4^{2-}), 100 mg of the resin was added and the extent of adsorption was determined in the natural pH of the solutions (no buffer) after 24 h.

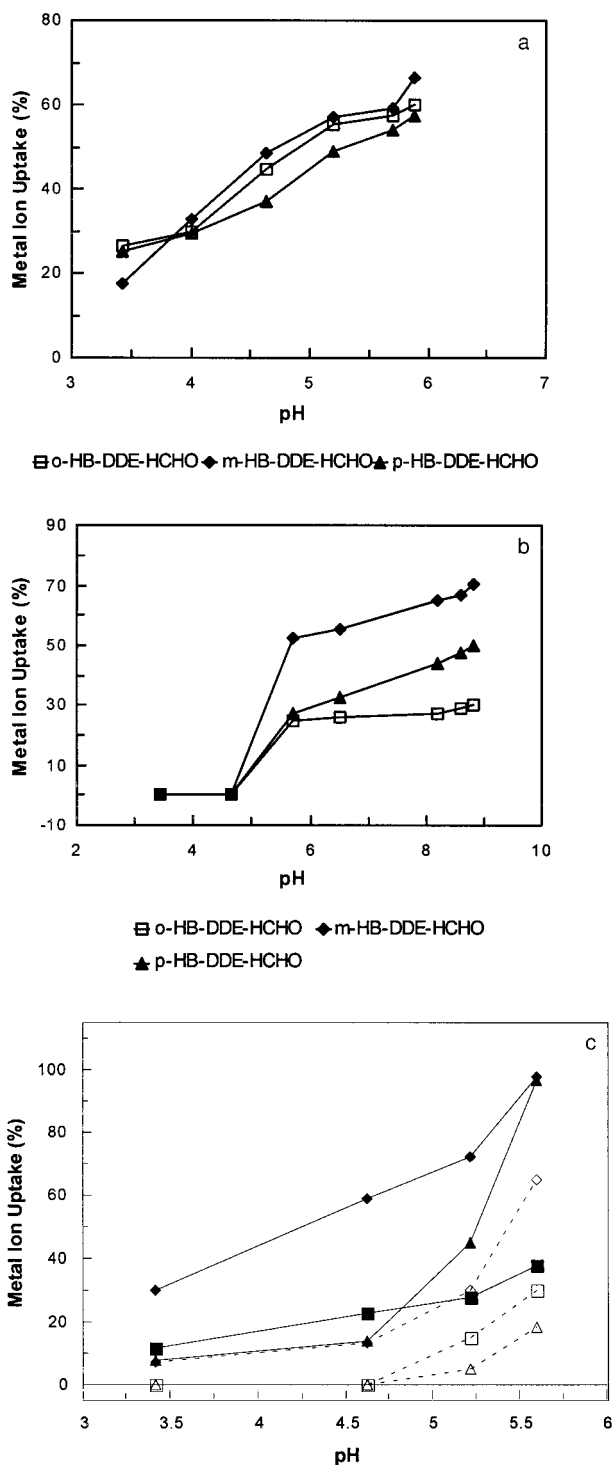


Figure 7 (a) Effect of pH on the adsorption of Cu(II): [Cu(II)]: 200 $\mu\text{g}/10$ mL, resin quantity: 100 mg, sorbent size: 100 mesh, buffer: $\text{CH}_3\text{COONa}/\text{CH}_3\text{COOH}$, temp. 30°C, contact time: 24 h. (b) Effect of pH on the adsorption of Ni(II): [Ni(II)]: 2000 $\mu\text{g}/10$ mL, resin quantity: 100 mg, sorbent size: 100 mesh, buffers: $\text{CH}_3\text{COONa}/\text{CH}_3\text{COOH}$ and $\text{NH}_4\text{OH}/\text{NH}_4\text{Cl}$, temp: 30°C, contact time: 24 h. (c) Effect of variation of solution pH on

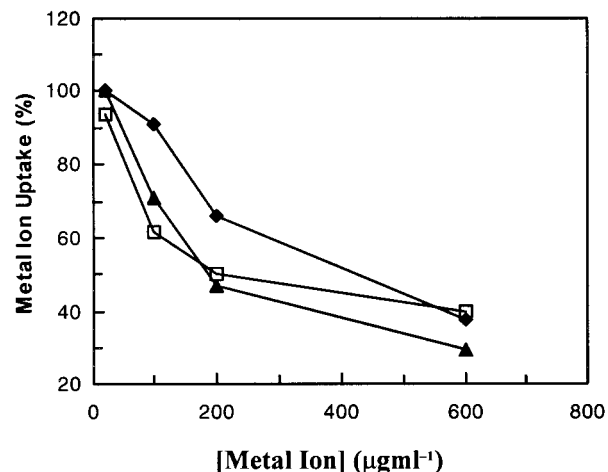


Figure 8 Effect of metal ion concentration: metal ion—Cu(II), volume of solution—10 mL, pH 5.6, resin quantity—100 mg, size—100 mesh, temp.—30°C, (■) *o*-, (◆) *m*-, and (□) *p*-HB-DDE-HCHO.

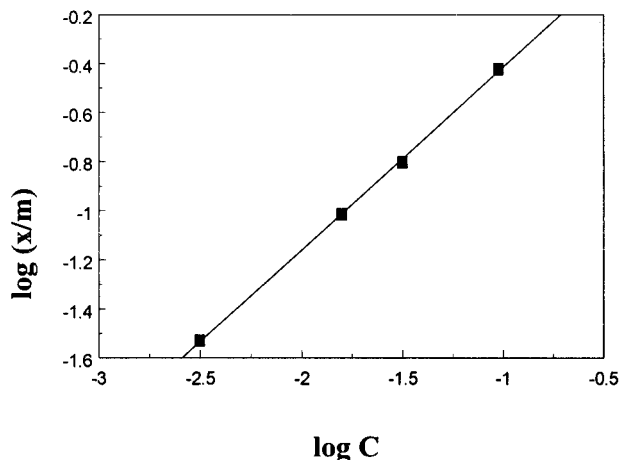
It was observed that the presence of alkali and alkaline earth metal ions and the accompanying anion have negligible effect on the adsorption behavior of the resins towards Cu(II) ions (Table IV).

Separation of Cu(II) from Ni(II)

Based on the sorption behavior of the resins at different pH values, the separation of Cu(II) and Ni(II) in a binary mixture was attempted. For this two sets of experiments were carried out. In the first case, 10 mL solution containing a fixed amount of Cu(II) (200 $\mu\text{g mL}^{-1}$) and varying amounts of Ni(II) (20 to 400 $\mu\text{g mL}^{-1}$) was treated with 100 mg of resin at a fixed pH for 24 h. It was seen that at pH 5.89 all three resins take up Cu(II) quantitatively and the adsorption of Ni(II) was negligible (Table V).

In another set of experiments, 10 mL solution containing 20 $\mu\text{g mL}^{-1}$ each of Cu(II) and Ni(II) was treated with 100 mg of resins at varying pH. It was seen that in the pH range 3.42–5.89, the sorbents *o*- and *p*-HB-DDE-HCHO exclusively adsorbed Cu(II), whereas *m*-HB-DDE-HCHO adsorbed mostly Cu(II) along with a small amount of Ni(II). For this resin, with increasing pH, the

metal ion uptake: sorbent size—100 mesh, quantity—100mg, time—24 h, temp—30°C, [M(II)] = 200 $\mu\text{g}/10$ mL, Cu(II) uptake by (■) *o*- (◆) *m*-, (▲) *p*-HB-DDE-HCHO, Ni(II) uptake by (□) *o*- (◇) *m*-, (△) *p*-HB-DDE-HCHO.

**Regression Output:**

Constant (k_{ad})	0.33225
Std Err of Y Est	0.01257
R Squared	0.99950
No. of Observations	4
Degrees of Freedom	2
X Coefficient(s)(1/n)	0.74626
Std Err of Coef.	0.01173

Figure 9 Freundlich adsorption isotherm: plot of $\log(x/m)$ vs. $\log C$ for determination of k_{ad} and n .

adsorption of copper reached nearly 100% with a many-fold increase in the K_d values, whereas the adsorption for Ni(II) remained at a nearly fixed value of about 25% (Table VI). Thus, it was concluded that while *o*-, *m*-, *p*-HB-DDE-HCHO resins are very efficient in adsorbing Cu(II) from a solution containing $200 \mu\text{g mL}^{-1}$ Cu(II) and varying amounts of Ni(II), the *o*- and *p*-HB-DDE-HCHO resins were suitable for selective separation of Cu(II) from Ni(II) at a lower Cu(II) concentration.

Deb and Rao,²⁹ in studying a polystyrene-divinylbenzene-based macroreticular resin functionalized with bis-(*N,N'*-salicylidine)1,3-propanedia-

mine Schiff-base ligand, observed that the resin could efficiently adsorb a number of metal ions. However, the resin demonstrated nearly identical preference for both Cu(II) and Ni(II) among other metal ions. In our case, resins derived from Schiff bases could be successfully employed to exclusively adsorb Cu(II) from a Cu(II)-Ni(II) mixture. Thus, there is a difference in selectivity of the Schiff bases when anchored to a preformed polymer and when present in the form of a polymeric segment. In the latter case, the type of molecular architecture renders the material to exhibit selectivity to certain specific metal ions, leading to their complete separation.

As a further extension of the work, the reusability of the resins immobilized on activated silica is being studied for other elements like Cr(VI), UO_2^{2+} by both batch and column methods. The

Table III Effect of Resin Quantity on Metal Ion Uptake^a

Resin	Resin Quantity (μg)	Metal Uptake (%)
<i>o</i> -HB-DDE-HCHO	50	25
	100	60
	200	51.66
	400	61.66
<i>m</i> -HB-DDE-HCHO	50	40
	100	60
	200	92.5
	400	100
<i>p</i> -HB-DDE-HCHO	50	22.5
	100	46
	200	55
	400	62.33

^a [Cu(II)] = $200 \mu\text{g mL}^{-1}$, sorbent size—100 mesh, pH—5.89, temp.— 30°C , contact time—24 h.

Table IV Effect of Added Salts on the Adsorption of Cu(II) Ion by the Resins^a

Resin	Cu(II) Uptake (%)			
	In the Absence of Added Salt	In the Presence of Added Salt		
		Na^+	K^+	Mg^{2+}
<i>o</i> -HB-DDE-HCHO	41.5	40.9	40.9	41.3
<i>m</i> -HB-DDE-HCHO	60.6	59.9	59.5	58.7
<i>p</i> -HB-DDE-HCHO	46.66	45	46.23	44.3

^a [Cu(II)]: $2000 \mu\text{g}/10 \text{ mL}$, resin quantity: 100 mg, sorbent size: 100 mesh, temp: 30°C , contact time: 24 h, [Cu(II)]: $4000 \mu\text{g}/10 \text{ mL}$, pH: natural, common anion: SO_4^{2-} .

Table V Separation of Cu(II) from Ni(II) with Increasing Ni(II) Concentration at Fixed pH^a

Resin	[M(II)] μgmL ⁻¹		Metal Uptake (%)	
	Cu(II)	Ni(II)	Cu(II)	Ni(II)
<i>o</i> -HB-DDE-HCHO	200	20	60.83	0
	200	50	34	0
	200	200	31	0
	200	400	29	6.2
<i>m</i> -HB-DDE-HCHO	200	20	63.3	0
	200	50	61.6	0
	200	200	60	5
	200	400	53	12.5
<i>p</i> -HB-DDE-HCHO	200	20	38	0
	200	50	35	0
	200	200	34	0
	200	400	31	5

^a Resin quantity—100 mg, size—100 mesh, pH—5.89, temp.—30°C, contact time—24 h.

preliminary results, reported elsewhere,^{12d} involving a structurally related resin, have been highly encouraging, demonstrated by a minimum of five efficient loading-stripping cycles.

CONCLUSIONS

Phenolic Schiff bases *o*-, *m*-, and *p*-HB-DDE could be condensed with formaldehyde to furnish a set of reactive polymers, which could form polyche-

lates readily with Cu(II) and Ni(II). The polyche-
lates were found to be thermally less stable than
the corresponding resins. The reduced stability
could be attributed to the presence of a large
number of solvent molecules either coordinated to
the metal ions and/or anchored to the resin ma-
trix. The polychelates were found to possess ap-
preciable crystallinity. The resins could be suc-
cessfully employed for the adsorption studies in-
volving Cu(II) and Ni(II). It was found that
m-HB-DDE-HCHO was more effective in adsorb-
ing these metal ions than *o*- and *p*-HB-DDE-
HCHO. This was attributed to a lower degree of
crosslinking, and a consequent ease of swelling
for *m*-HB-DDE-HCHO. The accessibility of the
coordination sites by the metal ions is considered
as a relatively more determining factor than the
ease of chelate ring formation. Although the more
reactive resin *m*-HB-DDE-HCHO was useful for
loading relatively large quantities of metal ions,
the less reactive *o*-HB-DDE-HCHO could be suc-
cessfully employed to efficiently separate Cu(II)
from Ni(II).

We are thankful to Prof. K. E. Geckeler of the Department of Materials Science and Engineering, K-JIST, South Korea, for many helpful discussions. We also thank the different Regional Sophisticated Instrumentation Centers located in India (Central Drug Research Institute, Lucknow; Punjab University, Chandigarh, IIT, Mumbai, and IIT, Chennai) for providing analytical facilities. We gratefully acknowledge the S. P. University, Gujrat, India, for providing GPC results.

Table VI Separation of Cu(II) from a Mixture of Cu(II) and Ni(II) at Varying pH

Resin	pH	Cu(II)		Ni(II)	
		Uptake (%)	<i>K</i> _d	Uptake (%)	<i>K</i> _d
<i>o</i> -HB-DDE-HCHO	3.42	10	1.11	0	0
	4.63	20	25	0	0
	5.2	35.5	55.03	0	0
	5.89	43.75	77.77	0	0
<i>m</i> -HB-DDE-HCHO	3.42	25	33.33	20	25
	4.63	62.5	166.66	25	33.33
	5.2	97	3233.3	26	35.15
	5.89	98	4900	25	33.33
<i>p</i> -HB-DDE-HCHO	3.42	0	0	0	0
	4.63	7.5	8.1	0	0
	5.2	35	53.84	0	0
	5.89	97	3233	0	0

^a [Cu(II)] = [Ni(II)] = 200 μg/10 mL, resin quantity: 100 mg, sorbent size: 100 mesh, temp: 30°C, contact time: 24 h.

REFERENCES

- Schmuckler, G. *Talanta* 1965, 12, 281; Blasius, E.; Brozio, B. In *Chelates in Analytical Chemistry*; Flaschka, H. A.; Barnard, A. J., Jr., Eds.; Marcel Dekker, Inc.: New York, 1967, p. 49, vol. 1; Mayasova, G. V.; Savvin, S. B. *Crit Rev Anal Chem* 1986, 17, 1; Kantipuly, C.; Katragadda, S.; Chow, A.; Gesser, H. D. *Talanta* 1990, 37, 491; Biswas, M.; Mukherjee, A.; *Adv Polym Sci* 1994, 115, 89.
- Riley, J. P.; Taylor, D. *Anal Chim Acta* 1968, 40, 479; Garg, B. S.; Sharma, R. K.; Bhojak, N.; Mittal, S. *Microchem J* 1999, 61, 94.
- Zigon, M.; Sebenik, A.; Osredkar, U.; *Vizovisek, I. Angew Makromol Chem* 1987, 148, 127.
- Zigon, M.; Sebenik, A.; Osredkar, U. *Makromol Sci Chem A* 1988, 25, 942.
- Parmer, J. S.; Patel, M. L.; Patel, M. N. *Angew Makromol Chem* 1981, 93, 1.
- Moyers, E. M.; Fritz, J. S. *Anal Chem* 1977, 49, 418.
- Lillin, H. V. *Angew Chem* 1954, 66, 649.
- De Geiso, R. C.; Donaruma, L. G.; Tomic, E. A. *J Appl Polym Sci* 1965, 9, 411.
- Sakaguchi, T.; Nakajima, A. *Sep Sci Technol* 1986, 21, 519.
- Hodgkin, J. H.; Eibl, R. *React Polym Ion Exch Sorbents* 1985, 3, 83.
- (a) Ueno, K.; Martell, A. E. *J Phys Chem* 1955, 59, 998; 1956, 60, 1270; (b) Okawa, H., et al. *J Chem Soc Dalton Trans* 1985, 59; (c) Sinn, E., et al. *Inorg Chem* 1985, 24, 127; (d) Collins, T. H., et al. *J Am Chem Soc* 1986, 108, 6593; (e) Che, C.-M.; Cheng, W.-K. *J Chem Soc Chem Commun* 1986, 1443.
- (a) Samal, S.; Das, R. R.; Sahoo, D.; Acharya, S.; Panda, R. L.; Rout, R. C. *J Appl Polym Sci* 1996, 62, 1437; (b) Samal, S.; Das, R. R.; Sahoo, D.; Acharya, S. *Polym Int* 1997, 44, 41; (c) Samal, S.; Mohapatra, N. K.; Acharya, S.; Dey, R. K. *Reactive and Functional Polymers*, to appear; (d) Samal, S.; Dey, R. K.; Acharya, S.; Mohapatra, N. K. *Proceedings of International Conference on Polymers Beyond AD 2000 (Polymers 99)*, New Delhi, January 1999.
- Yang, C.-P.; Chen, W.-T. *J Polym Sci Part A Polym Chem* 1994, 32, 1101.
- Chen, H.; Cronin, J. A.; Archer, R. D. *Macromolecules* 1994, 27, 2174.
- Thamizharasi, S.; Reddy, A. V. R. *Polymer* 1992, 33, 2421.
- Oriel, L.; Alonso, P. J.; Martineoz, J. I.; Pinol, M.; Serrano, J. L. *Macromolecules* 1994, 27, 1869.
- Nakamoto, K.; Fujita, J.; Tanaka, S.; Kobayashi, M. *J Am Chem Soc* 1957, 79, 4904.
- Gatehouse, B. M.; Livingston, S. E.; Nyholm, R. S. *J Chem Soc* 1957, 4222.
- Chiang, W.; Mei, W. *Eur Polym J* 1993, 29, 1047.
- Lever, A. B. P. *Coord Chem Rev* 1968, 3, 119.
- Coats, A. W.; Redfern, J. P. *J Polym Sci Polym Lett Ed* 1965, 3, 921.
- Van Krevelen, D. W.; Van Heerden, C.; Humfjens, F. J. *Fuel* 1951, 30, 253.
- Broido, A. *J Polym Sci Polym Lett Ed A2*, 1969, 7, 1761.
- Bassett, J.; Denney, R. C.; Jeffery, G. H.; Mendham, J. In *Vogel's Text Book of Quantitative Analysis*; Longman: New York, 1978, p. 156, 4th ed.
- Lezzi, A.; Cobianco, S. *J Appl Polym Sci* 1994, 54, 889.
- Tikhomirova, T. I.; Fadeeva, V. I.; Kubryavtsev, G. V.; Nesterenko, P. N.; Ivanov, V. M.; Savitchev, A. T.; Smirnova, N. S. *Talanta* 1991, 38, 267.
- Luo, X.; Su, Z.; Gao, W.; Zhang, G.; Chang, X. *Analyst* 1992, 117, 145.
- Feng, M.; Does, L. V. D.; Bantjes, A. *J Appl Polym Sci* 1994, 52, 21.
- Dev, K.; Rao, G. N. *Analyst* 1995, 120, 2509.